Drug Delivery

ISSN: 1071-7544 (Print) 1521-0464 (Online) Journal homepage: https://www.tandfonline.com/loi/idrd20

# Nanostructured lipid carriers, solid lipid nanoparticles, and polymeric nanoparticles: which kind of drug delivery system is better for glioblastoma chemotherapy?

Jie Qu, Liangqiao Zhang, Zhihua Chen, Guohua Mao, Ziyun Gao, Xianliang Lai, Xingen Zhu & Jianming Zhu

**To cite this article:** Jie Qu, Liangqiao Zhang, Zhihua Chen, Guohua Mao, Ziyun Gao, Xianliang Lai, Xingen Zhu & Jianming Zhu (2016) Nanostructured lipid carriers, solid lipid nanoparticles, and polymeric nanoparticles: which kind of drug delivery system is better for glioblastoma chemotherapy?, Drug Delivery, 23:9, 3408-3416, DOI: 10.1080/10717544.2016.1189465

**To link to this article:** https://doi.org/10.1080/10717544.2016.1189465

Drug Delivery

http://informahealthcare.com/drd
ISSN: 1071-7544 (print), 1521-0464 (electronic)

Drug Deliv, 2016; 23(9): 3408–3416
 DOI: 10.1080/10717544.2016.1189465

Taylor & Francis
Taylor & Francis Group

RESEARCH ARTICLE

# Nanostructured lipid carriers, solid lipid nanoparticles, and polymeric nanoparticles: which kind of drug delivery system is better for glioblastoma chemotherapy?

Jie Qu*, Liangqiao Zhang*, Zhihua Chen, Guohua Mao, Ziyun Gao, Xianliang Lai, Xingen Zhu, and Jianming Zhu

*Department of Neurosurgery, Second Affiliated Hospital, Nanchang University, Nanchang, Jiangxi, China*

**Abstract**

*Context*: Glioblastoma is a malignant brain tumor originating in the central nervous system. Successfully therapy of this disease required the efficient delivery of therapeutic agents to the tumor cells and tissues. Delivery of anticancer drugs using novel nanocarriers is promising in glioma treatment.

*Objective*: Polymeric nanoparticles (PNPs), solid lipid nanoparticles (SLNs), and nanostructured lipid carriers (NLCs) were constructed for the delivery of temozolomide (TMZ). The anti-tumor effects of the three kinds of nanocarriers were compared to provide the optimum choice for gliomatosis cerebri treatment.

*Methods*: TMZ-loaded PNPs (T-PNPs), SLNs (T-SLNs), and NLCs (T-NLCs) were formulated. Their particle size, zeta potential, drug encapsulation efficiency (EE), and drug loading (DL) capacity were evaluated. Anti-tumor efficacies of the three kinds of nanocarriers were evaluated on U87 malignant glioma cells (U87 MG cells) and mice-bearing malignant glioma model.

*Results*: T-NLCs displayed the best anti-tumor activity than other formulations *in vivo* and *in vitro*. The most significantly glioma inhibition was observed on NLCs formulations than PNPs and SLNs.

*Conclusion*: This work demonstrates that NLCs can deliver TMZ into U87MG cells more efficiently, with higher inhibition efficacy than PNPs and SLNs. T-NLCs could be an excellent drug delivery system for glioblastoma chemotherapy.

**Keywords**

Glioblastoma chemotherapy, nanostructured lipid carriers, polymeric nanoparticles, solid lipid nanoparticles, temozolomide

**History**

Received 17 March 2016
Revised 3 May 2016
Accepted 10 May 2016

## Introduction

Glioblastoma multiforme (GBM), the most common malignant central nervous system tumor, is highly aggressive with a 5-year survival rate lower than 5% (Gao et al., 2014). Under the standard treatment regimen, including resection followed by radiotherapy and chemotherapy [typically temozolomide (TMZ)], GBM patients can expect a median survival of 14.6 months (Hou et al., 2006). However, the poor prognosis can still be a troublesome, resulting from limited delivery of therapeutics across the blood–brain barrier (BBB), therapeutic resistance, and a high possibility of recurrence (Woodworth et al., 2014; Kim et al., 2015). Thus, there is a critical need for means to cross the BBB and improve the efficacy of current GBM therapies.

Drug delivery remains a critical barrier to the treatment of central nervous system (CNS) tumors such as GBM. Based on the nanotechnology such as liposome, polymeric nanoparticles (PNPs), solid lipid nanoparticles (SLNs), and nanostructured lipid carriers (NLCs), recent research efforts have been aimed to targeting drugs to the brain (Chekhonin et al., 2012; Zhang et al., 2013; Carbone et al., 2014; Gastaldi et al., 2014; Song et al., 2016). Compared with conventional drug formulations, carefully designed nano-formulations offer significant advantages such as improved drug solubility, facilitation of drug delivery across the BBB, selective targeting, and reduced side effects (Jain, 2010; Kim et al., 2015).

Nanoparticles (NPs) in particular are very interesting for drug delivery purposes for their versatility. The potential mechanism of NPs-mediated drug delivery across the BBB is determined by the chemistry, architecture, and properties of the NPs (Barbu et al., 2009). Common NPs would be rapidly cleared from the blood circulation by the reticulo-endothelial system (RES), and severely limit the utility of NPs in targeting drugs to the CNS. Several strategies have been established to overcome this hurdle: designing longer-circulating NPs (''stealth NPs'') and surface coating with hydrophilic polymers/surfactants (Moghimi et al., 2001; Gastaldi et al., 2014). For instance, Polysorbate 80-coated

*These authors contributed equally to this work.

Address for correspondence: Jianming Zhu, Department of Neurosurgery, Second Affiliated Hospital, Nanchang University, No. 1 Minde Road, Donghu District, Nanchang City 330000, Jiangxi Province, People's Republic of China. Email: zhujmncu@163.com

polybutylcyanoacrylate (PBCA) NPs were able to deliver TMZ to the brain with a superior rate compared with TMZ solution and TMZ NPs non-coated with Polysorbate 80 (Tian et al., 2011).

The use of lipids as matrices for the preparation of lipid nanoparticles such as SLNs or NLCs guarantees many advantages with respect to other materials, in particular: good biocompatibility, low cytotoxicity, and controlled drug release (Müller et al., 2011). SLNs are frequently proposed as drug delivery systems for various compounds targeted to the CNS because of the following advantages: stabilizing drugs that suffer from physicochemical or biological instability; improving the bioavailability of drugs that cross the BBB; increasing permeating of drugs through the BBB (Gastaldi et al., 2014). Huang et al. compared the pharmacokinetics and biodistribution of TMZ delivered by SLNs with common TMZ solution, using mice as an animal model. The results showed that T-SLNs increased significantly the drug brain targeting efficiency: 6.76% for TMZ solution and 13.25% for T-SLNs (Huang et al., 2008).

NLCs, the new generation of SLNs, are composed of solid lipids and liquid lipids leading to a crystal structure with more imperfections and, therefore, with more drug loading. Recently, our group dedicated to designing NLCs as the carrier for drug delivery for the treatment of glioma. For instance, arginine–glycine–aspartic acid peptide (RGD) modified NLCs were used for the delivery of TMZ for gliomatosis cerebri treatment (Song et al., 2016). NLCs were constructed and used for the co-delivery of vincristine and TMZ to glioma (Wu et al., 2015). TMZ and DNA co-encapsulated NLCs were engineered to evaluate the *in vivo* therapeutic effect for GBM, using mice as an animal model. The results demonstrated that TMZ/DNA-NLCs transfer both drug and gene into the gliomatosis cerebri, enhance the anti-tumor capacity and gene transfection efficacy (Chen et al., 2016).

On the basis of the previous studies of our group (Wu et al., 2015; Chen et al., 2016; Song et al., 2016), this work aimed to the preparation of different nanocarriers (PNPs, SLNs, and NLCs) to select the ideal carrier with the most adequate physic-chemical and technological properties for the delivery of TMZ for the treatment of GBM. For the purpose, it was studied the *in vitro* cytotoxicity on U87 malignant glioma cells (U87 MG cells), *in vivo* biodistribution behavior and *in vivo* anti-tumor efficiency on mice-bearing malignant glioma model.

## Materials and methods

### Materials

TMZ was kindly provided by Laimei Pharmaceutical Co., Ltd (Chongqing, China). Stearic acid, poly-(lactic-*co*-glycolic acid) (PLGA, molar ratio of D,L-lactic to glycolic acid, 50:50) was purchased from Ji'nan Daigang Biotechnology Co. Ltd (Ji'nan, China). Tween-80, poly (vinyl alcohol) (PVA, 87–89% hydrolyzed, *M*w 13 000–23 000), dimethyldioctadecylammonium bromide (DDAB), (3-[4,5-dimehyl-2-thiazolyl]-2,5-diphenyl-2*H*-tetrazolium bromide (MTT), and soybean phosphatidylcholine (SPC) were purchased from Sigma Aldrich (St. Louis, MO). Distearoyl phosphatidylethanolamine (DSPE) was purchased from Avanti Polar Lipids (Alabaster, AL). COMPRITOL® 888 ATO (888 ATO) was generously provided by Gattefossé (Paramus, NJ). Polyoxyl castor oil (Cremophor ELP) was donated by BASF (Ludwigshafen, Germany). Injectable soya lecithin was obtained from Shanghai Taiwei Pharmaceutical Co, Ltd (Shanghai, China). All other chemicals were of analytical grade or higher.

### Animals and cells

U87 MG cells were obtained from the American type culture collection (Manassas, VA) and cultured in Dulbecco's Modified Eagle's Medium (DMEM) (Sigma, St. Louis, MO) supplemented with 10% fetal bovine serum (FBS) (Fisher Chemicals, Fairlawn, NJ) in a 5% $CO_2$ fully humidified atmosphere.

BALB/c nude mice (5–6-week-old, 18–22 g) were purchased from the Shanghai Slack Laboratory Animal Co., Ltd. (Shanghai, China). All animal experiments complied with the Animal Management Rules of the Ministry of Health of the People's Republic of China.

### Preparation

#### *Preparation of T-PNPs*

T-PNPs were prepared by a solvent displacement technique (Zou et al., 2009). Briefly, 200 mg of PLGA and 50 mg TMZ were accurately weighted and dissolved in 5 mL acetone to form the organic phase. The organic phase was added dropwise into a desired aqueous stabilizer of either 1% PVA (w/v) being stirred at 400 rpm by a laboratory magnetic stirrer (ETS-D4 stirrer, IKA, Staufen, Germany) at room temperature for 4 h. Then the resulting suspension was then dispersed with Milli-Q water and then dialyzed against Milli-Q water for 24 h to get the T-PNPs suspension. The T-PNPs suspension was washed using Milli-Q water twice and resuspended in phosphate-buffered saline (PBS pH 7.4), filtered through a membrane with 0.45 μm pore size (25 mm filter, Phenomenex, Torrance, CA). Blank PNPs were prepared using the same method without adding TMZ.

#### *Preparation of T-SLNs*

T-SLNs were prepared following the solvent displacement technique (Wang et al., 2012). Stearic acid (100 mg) and injectable soya lecithin (50 mg) were accurately weighted and dissolved in 10 mL acetone. The organic phase was added drop-wise, into the 1% DDAB (w/v) solution, which was being stirred at 600 rpm at room temperature. Then the resulting suspension was then dispersed with Milli-Q water and then dialyzed against Milli-Q water for 24 h to get the T-SLNs suspension. The T-SLNs suspension was washed using Milli-Q water twice and resuspended in PBS (pH 7.4), filtered through a membrane with 0.45 μm pore size (25 mm filter, Phenomenex, Torrance, CA). Blank SLNs were prepared using the same method without adding TMZ.

#### *Preparation of T-NLCs*

T-NLCs were prepared by solvent diffusion method (Tiwari & Pathak, 2011). In brief, the lipid dispersion was composed of 888 ATO (200 mg), Cremophor ELP (200 mg), and SPC

(200 mg). Injectable soya lecithin (100 mg) and TMZ (50 mg) were dissolved in 1 mL of dimethyl formamide (DMF) and added to the lipid dispersion with heating at the temperature of 80–85 °C to form the lipid phase. Aqueous phase was prepared by Tween-80 and 0.5% DDAB (w/v) in 10 mL of water. This aqueous solution was then stirred and heated to 30 °C. The lipid phase was rapidly injected into the stirred aqueous phase (800 rpm) at 30 °C, and the resulting suspension was then dispersed with Milli-Q water and then dialyzed against Milli-Q water for 24 h to get the T-NLCs suspension. The T-NLCs suspension was washed using Milli-Q water twice and resuspended in PBS (pH 7.4), filtered through a membrane with 0.45 μm pore size (25 mm filter, Phenomenex, Torrance, CA). Blank NLCs were prepared using the same method without adding TMZ. The obtained T-PNPs, T-SLNs, and T-NLCs were stored at 2–8 °C.

## Characterization

### *Surface morphology*

The surface morphology of T-PNPs, T-SLNs, and T-NLCs was investigated using transmission electron microscopy (TEM, JEM-1400; JEOL Ltd., Tokyo, Japan) (Wang et al., 2016). Three samples for testing were prepared, respectively, by placing a drop of nanoparticle suspension onto a copper grid and air drying, followed by negative staining with one drop of 3% aqueous solution of sodium phosphotungstate for contrast enhancement. The air-dried samples were then directly examined under the TEM.

### *Particle size and zeta potential*

The mean particle size, size distribution, and zeta potential of T-PNPs, T-SLNs, and T-NLCs were determined by using the Malvern Zetasizer Nano ZS (Malvern Instrument Ltd., Worcestershire, UK) (Khan et al., 2015). The average particle size was expressed as volume mean diameter.

### *Drug encapsulation and drug-loading efficiency*

The drug encapsulation efficiency (EE) and drug loading (DL) efficiency of three kinds of formulations were measured by using the HITACHI P-4010 inductively coupled plasma mass spectrometry (ICP-MS) (Hitachi Ltd, Kyoto, Japan). Briefly, 5 mL formulations were centrifuged (16 000 rpm and 4 °C for 30 min) separately, and the supernatants were then determined using the ICP-MS. The EE and the DL were expressed as the percentage of the amount of TMZ encapsulated in the NLCs to the total amount of TMZ initially used. EE were calculated as

$$\text{EE}\ (\%) = \text{Concentration of (total TMZ} - \text{free TMZ)}/\text{Concentration of total TMZ} \times 100.$$

$$\text{DL}\ (\%) = \text{Concentration of (total TMZ} - \text{free TMZ)}/\text{Concentration of total TMZ and carriers} \times 100.$$

## Serum stability

Serum stability of T-PNPs, T-SLNs, and T-NLCs was evaluated in fetal bovine serum (FBS). The formulations were incubated in phosphate buffered solution (PBS) containing 50% FBS (v/v) at 37 °C for 24 h, separately. At scheduled times (0, 2, 4, 8, 12, and 24 h), 1 mL of each sample was diluted with 2 mL THF and the mixture was bath sonicated for 5 min, followed by centrifugation at 10 000 rpm for 5 min. The variation trends of the size and EE were calculated by the same method mentioned in the above section.

## *In vitro* drug release

The release of T-PNPs, T-SLNs, T-NLCs, and free TMZ solution (T-SOL) was evaluated by the dialysis method. Briefly, samples were added to the dialysis bag separately. Then, the dialysis bags were incubated with 30 ml of release medium (PBS, pH 7.4) at 37 °C with stirring at 100 rpm. At the predetermined time intervals, 1 ml of solution was removed, and 1 ml of fresh medium was filled to replace the remaining release medium. The amount of TMZ released from the samples was then determined by the same method described above.

## *In vitro* cytotoxicity

The cytotoxicity of T-PNPs, T-SLNs, and T-NLCs was tested in U87 MG cells using the MTT assay (Zhang et al., 2016). Briefly, cells were seeded in a 96-well plate at a density of $1 \times 10^4$ cells/well and allowed to adhere for 24 h prior to the assay. Cells were exposed to various TMZ concentrations (0.1, 0.5, 1, 5, and 10 μM) of T-SOL, blank PNPs, blank SLNs, blank NLCs, T-PNPs, T-SLNs, and T-NLCs, respectively. Culture medium was used as a blank control. After 48 h of incubation, MTT solution (5 mg/mL) was added to each well and the cells were incubated for another 4 h. Cellular viability was assessed according to the procedures of the MTT manufacturer and the absorbance at 570 nm was measured using a microplate reader (Model 680, Bio-Rad Laboratories Inc., Philadelphia, PA). Cells without the addition of MTT reagents were used as a blank control. The drug concentration causing 50% inhibition ($IC_{50}$) was calculated determining the equation of the curve plotted between the two points of viability which includes the 50% (Martins et al., 2013; Kumar et al., 2016).

## *In vivo* anti-tumor efficacy

BALB/c nude mice were housed at a temperature of 25 ± 2 °C and a relative humidity of 70 ± 5% under natural light/dark conditions for 1 week before dosing. Then the mice were inoculating subcutaneously (s.c.) in the right armpit with U87 MG cells suspended in PBS for 24 h for the preparation of malignant glioma-bearing animal models. Mice were then divided into eight groups (six mice per group). The 0.9% sodium chloride solution (control), blank PNPs, blank SLNs, blank NLCs, T-SOL, T-PNPs, T-SLNs, and T-NLCs were prepared and then injected intravenously into the mice via the tail vein (i.v.). The initial day of i.v. administration was defined as day 0, and administration was then repeated once every 3 d (d) over a 21-d therapeutic period. The tumor growth was determined by caliper measurement every 3 d. The measurements were taken in two perpendicular dimensions and tumor volumes ($mm^3$) were calculated by applying

the formula $(L \times W^2)/2$, where $L$ is the longest dimension and $W$ is the dimension perpendicular to $L$. The anti-tumor efficacy of each formulation was evaluated by tumor inhibition rate, and was calculated using the following formula: tumor inhibition rate $(\%) = (Wc - Wt)/Wc \times 100$. $Wt$ and $Wc$ represent the mean tumor weight of the treated and control groups, respectively.

### Statistical analysis

Quantitative data were presented as means ± standard deviation (SD). Statistical significance was analyzed using Student's $t$-test or one-way ANOVA with the $p$ value less than 0.05 ($p < 0.05$) indicating significance.

## Results

### Characterization

*Surface morphology*

TEM images showed the surface morphology of T-PNPs, T-SLNs, and T-NLCs (Figure 1). The images of three kinds of carriers revealed nano-sized, spherical shape. The image of T-PNPs was white solid ball while T-SLNs were black solid ball. T-NLCs had a gray coat on the surface of the darker inside particle. According to the 100 nm bars in the images, the T-PNPs, T-SLNs, and T-NLCs were around 100 nm.

*Particle size, zeta potential, EE, and DL*

The particle size, size distribution, zeta potential, EE, and DL of all kinds of formulations were summarized in Table 1. The size of T-PNPs, T-SLNs, and T-NLCs was 108 nm, 95 nm, and 121 nm, respectively. The zeta potential of T-PNPs was negative (–28 mV); however, the potential of T-SLNs (+41 mV) and T-NLCs (+29 mV) was positive. The EE of T-PNPs, T-SLNs, and T-NLCs was over 80%. The DL of different formulations varies from 5.2% to 10.8%.

### Serum stability

Changes in size and EE in the presence of serum are described in Figures 2 and 3. All the three kinds of formulations were stable up to 24 h without any significant size or EE changes. Thus, T-PNPs, T-SLNs, and T-NLCs were considered very stable after incubation with FBS and suggest that this formulation will not aggregate or disassemble after intravenous administration.

### *In vitro* drug release

Figure 4 showed the release profile of TMZ from T-PNPs, T-SLNs, T-NLCs, and T-SOL. As indicated in the figure, burst release was observed on T-SOL, but no burst release was observed on the other three formulations. The release rate of T-PNPs was the slowest. The release of the T-SLNs was relatively faster than T-NLCs. The sustained release behavior of the carriers may give continuous protection of the drug and lead to the persistent therapeutic effect.

### *In vitro* cytotoxicity

Figure 5 shows the cytotoxicity of T-PNPs, T-SLNs, T-NLCs, and T-SOL in U87 MG cells at different concentrations after 48 h of incubation. All drug containing formulations inhibited the growth cells over the studied concentrations and the toxicity conformed to a concentration-dependent pattern. T-PNPs, T-SLNs, and T-NLCs showed significantly higher cytotoxicity than T-SOL ($p < 0.05$). The $IC_{50}$ values of T-SOL, T-PNPs, T-SLNs, and T-NLCs were 9.12, 4.86, 2.93, and 0.78 μM, respectively. The $IC_{50}$ value of T-NLCs was 4 and 7 times dose advantages over T-SLNs and T-PNPs,

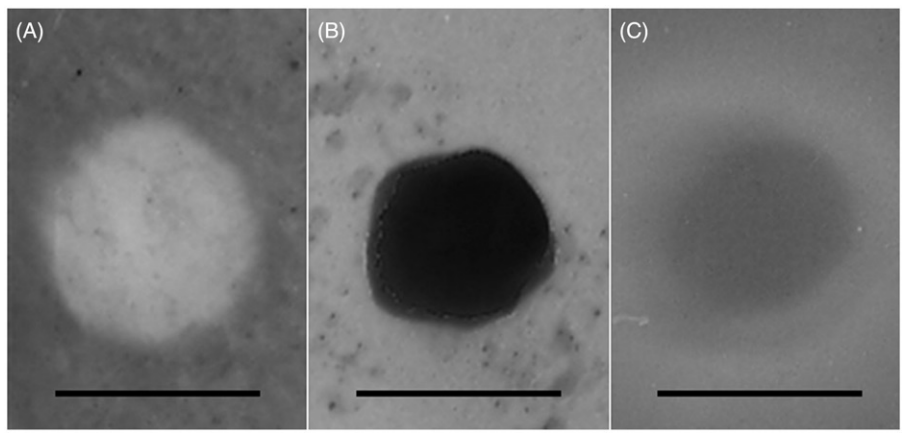


Figure 1. Surface morphology of T-PNPs, T-SLNs, and T-NLCs, bars mean 100 nm.

Table 1. Characterization of different vectors.

| Formulations | Particle size (nm) | Size distribution (PDI) | Zeta potential (mV) | EE (%) | DL (%) |
|---|---|---|---|---|---|
| PNPs | 108.2 ± 3.6 | 0.13 ± 0.03 | –31.2 ± 3.6 | N/A | N/A |
| SLNs | 93.8 ± 2.7 | 0.11 ± 0.02 | +37.6 ± 4.8 | N/A | N/A |
| NLCs | 123.6 ± 4.7 | 0.19 ± 0.05 | +28.5 ± 2.9 | N/A | N/A |
| T-PNPs | 109.1 ± 4.3 | 0.17 ± 0.04 | –28.2 ± 3.1 | 83.6 ± 3.2 | 10.8 ± 1.1 |
| T-SLNs | 94.6 ± 3.1 | 0.12 ± 0.03 | +41.2 ± 4.1 | 82.3 ± 2.8 | 9.6 ± 0.9 |
| T-NLCs | 121.4 ± 5.6 | 0.21 ± 0.06 | +29.1 ± 2.4 | 81.4 ± 3.7 | 5.2 ± 0.6 |

respectively. T-NLCs showed the best ability in reducing the viability of malignant glioma cells.

### *In vivo* anti-tumor efficacy

Figure 6 illustrates that the *in vivo* anti-tumor efficiency was evaluated in U87 MG solid tumors in mice. Although tumor growth was suppressed to some extent after the administration of T-SOL, while in contrast, tumor growth was significantly inhibited when nanocarrier formulations were administered intravenously. The most obvious tumor regressions were observed in the T-NLCs group, the tumor growth was prominently inhibited, which attained only 183 $mm^3$ on day 21, while tumor volume of the saline-treated group grew rapidly to 1192 $mm^3$ during 21-d therapeutic period. The tumor volume of T-PNPs and T-SLNs solution-treated groups reached to 656 and 487 $mm^3$, respectively. These results indicate that tumor growth was significantly inhibited by T-NLCs ($p < 0.05$). At 21 d of administration, the tumor inhibition rates of tumor-bearing mice treated with T-NLCs, T-SLNs, T-PNPs, and T-SOL were 85%, 59%, 45%, and 27% compared with control, respectively. T-NLCs inhibited tumor growth 1.4 or 1.8 times higher than T-SLNs or T-PNPs *in vivo*.

## Discussion

The present work aimed at the preparation of different nanocarriers (PNPs, SLNs, and NLCs) to select the ideal carrier with the most adequate physicochemical and technological properties for the delivery of TMZ for the treatment of GBM.

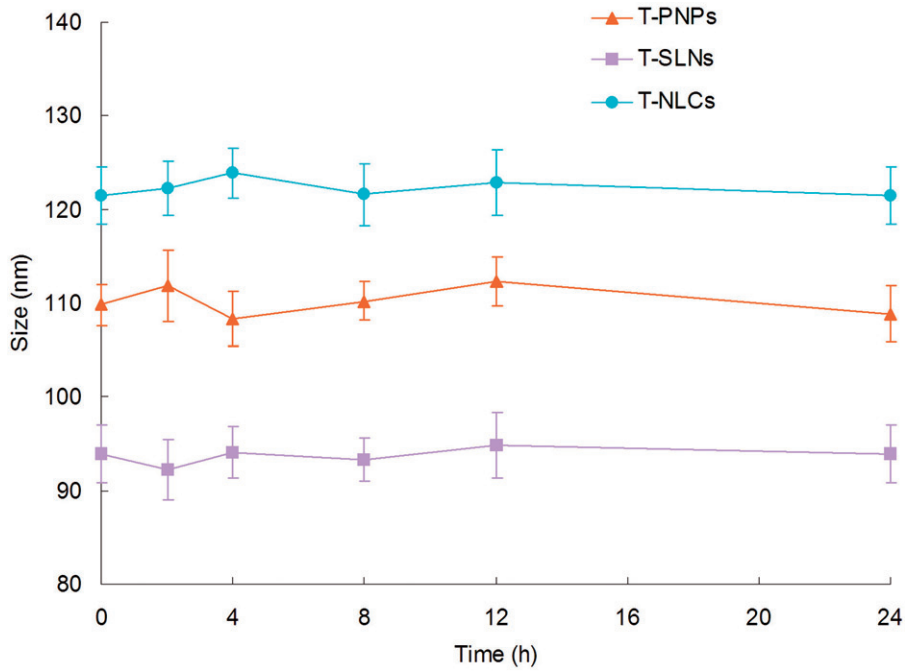


Figure 2. Changes in size of T-PNPs, T-SLNs, and T-NLCs in the presence of serum.

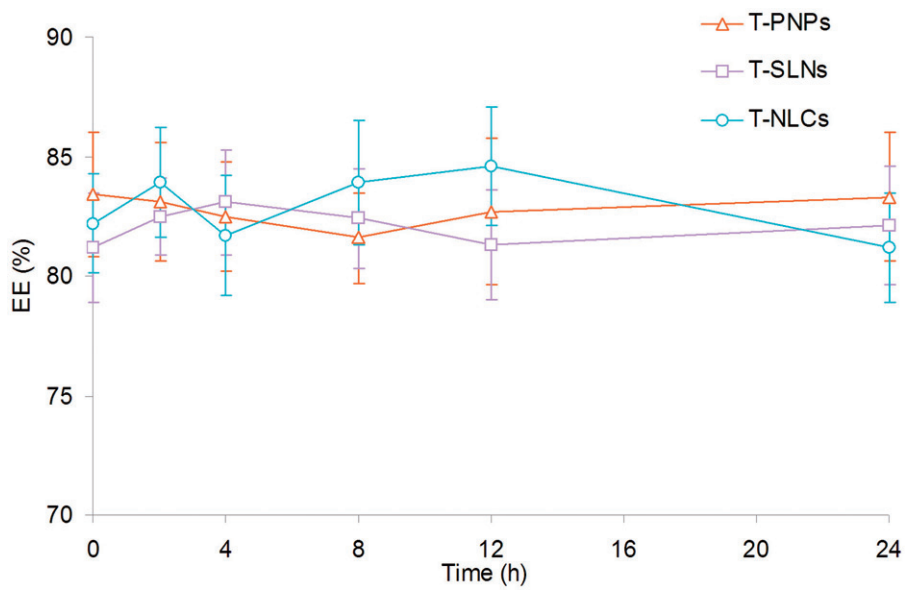


Figure 3. Changes in EE of T-PNPs, T-SLNs, and T-NLCs in the presence of serum.

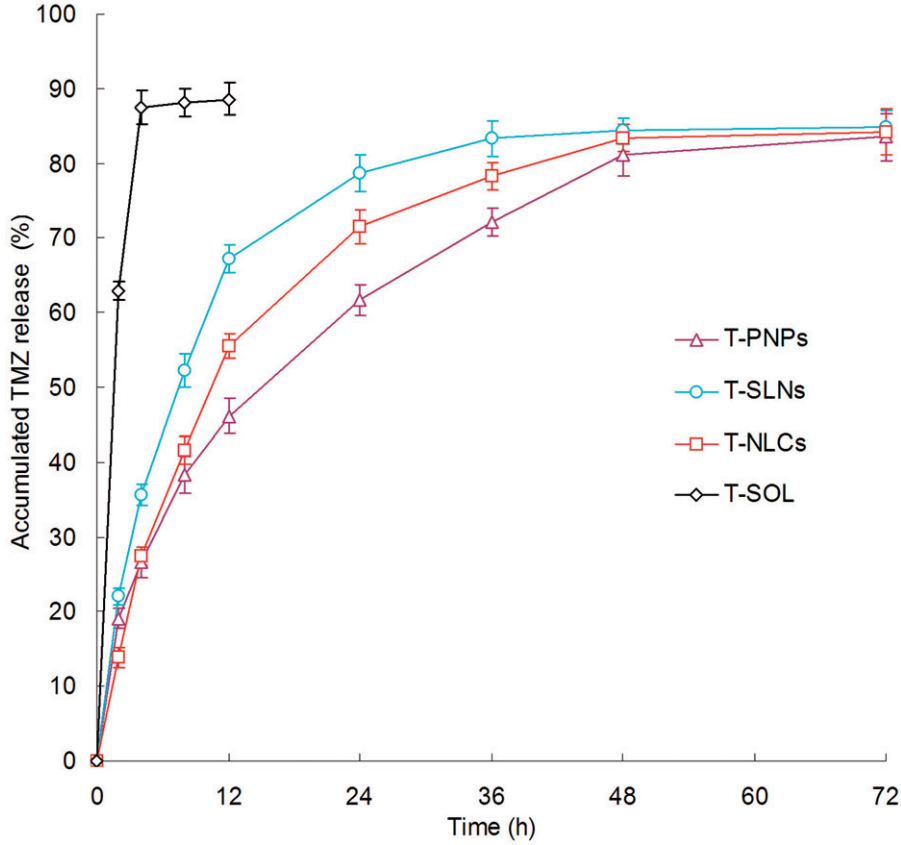


Figure 4. *In vitro* release profile of TMZ from T-PNPs, T-SLNs, T-NLCs, and T-SOL.

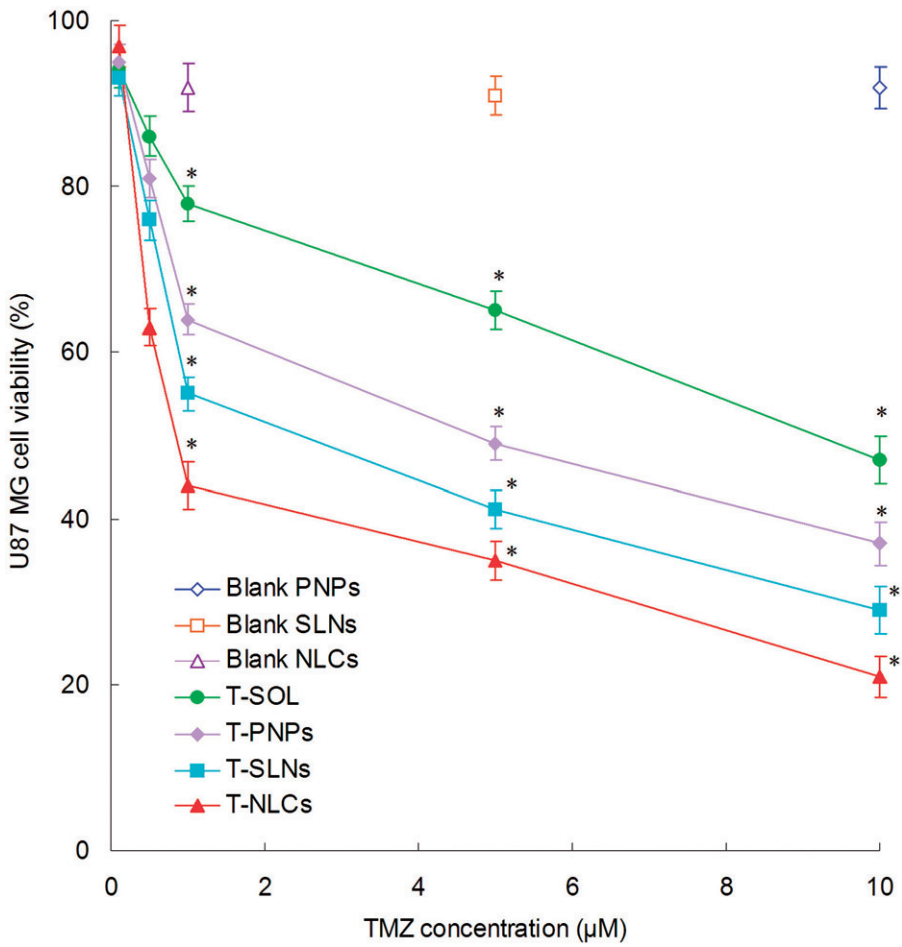


Figure 5. *In vitro* cytotoxicity of T-PNPs, T-SLNs, T-NLCs, and T-SOL in U87 MG cells. Statistical significance is shown by $*p < 0.05$, compared with relevant controls.

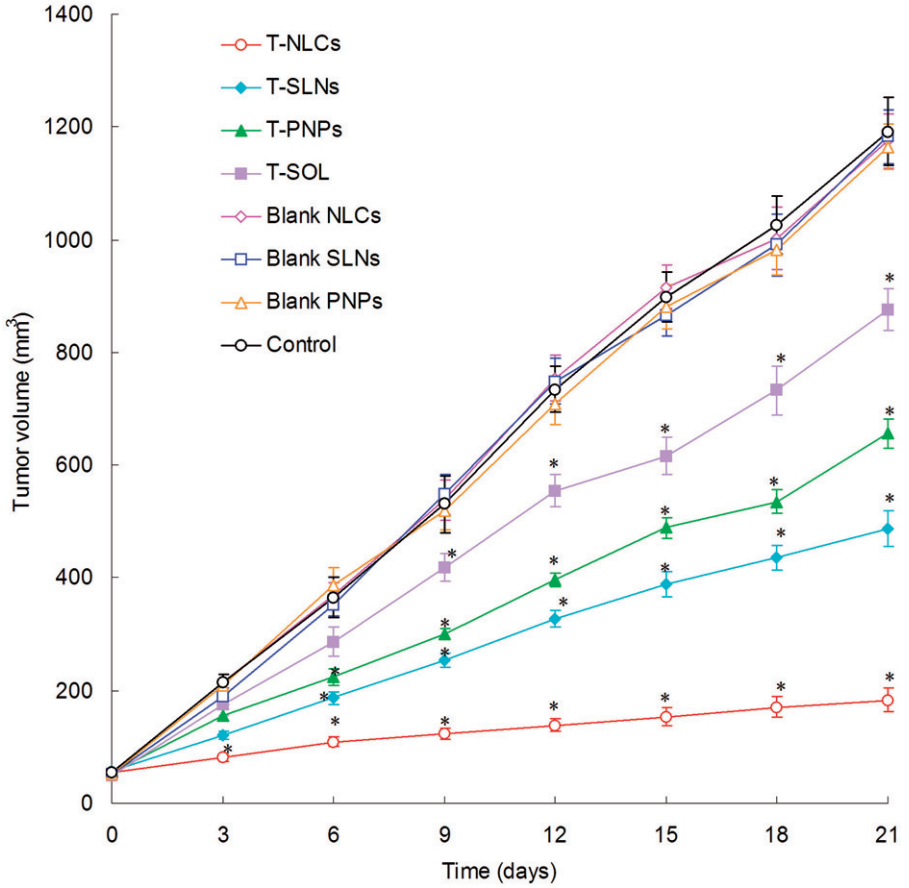


Figure 6. *In vivo* anti-tumor efficiency of T-PNPs, T-SLNs, T-NLCs, and T-SOL in U87 MG-bearing mice. Statistical significance is shown by $*p < 0.05$, compared with relevant controls.

The surface morphology of T-PNPs, T-SLNs, and T-NLCs revealed spherical shape (Figure 1). The image of T-PNPs was white solid ball while T-SLNs were black solid ball. T-NLCs had a gray coat on the surface of the darker inside particle. The differences in morphology and color of carriers may occur as a result of different compositions of lipid and surfactants used (Hejri et al., 2013). The size of T-PNPs, T-SLNs, and T-NLCs was around 100 nm. The zeta potential of T-PNPs was negative; however, the potential of T-SLNs and T-NLCs was positive. It is reported that the surface charge and the particle size of nanocarriers were important for efficient drug delivery: suitable particle size and zeta potential of the delivery system may enhance the bioavailability of bioactive compounds, adhesion efficiency with biological cells, and cellular uptake ability of the drug delivery system (Chinaeke et al., 2015). Cationic nanoparticles have been shown to keenly associate with negatively charged lipid bilayers, to be internalized rapidly, and enter cells via alternative mechanisms compared with anionic NPs (Boyles et al., 2015). A more likely explanation is the increased affinity of cationic nanoparticles for the negatively charged cell membrane. Besides uptake rates, surface charge also influences the intracellular trafficking (Agirre et al., 2015). It is considered that cationic NPs present within a lysosome undergoing acidification may accumulate protons entering via the proton pump, therefore, acting as a ''proton sponge'' and maintaining the pump active, resulting in osmotic swelling, lysis, and release of the lysosome content into the cytoplasm. The ability of encapsulating and loading of drugs is quite important for the delivery systems (Puglia et al., 2016). The good DL efficiency of carriers along with the suitable release behavior of the system could bring about high anti-tumoral activity to the delivery system (Frungillo et al., 2009).

Serum stability of T-PNPs, T-SLNs, and T-NLCs was evaluated in 50% FBS. Changes in size and EE in the presence of serum were described in. All the three kinds of formulations were stable up to 24 h without any significant size or EE changes (Figures 2 and 3). The results illustrated that these carriers were considered very stable after incubation with FBS and suggested that this formulation will not aggregate or disassemble after intravenous administration.

*In vitro* drug release profile shown that the TMZ release from T-PNPs, T-SLNs, and T-NLCs in a sustained manner (Figure 4). Using nano-sized drug carriers for the delivery of insoluble drugs is the easiest way to improve the solubility and stability of anticancer drugs (Anirudhan & Binusreejayan, 2016). The drug release may be controlled by diffusion, swelling, and/or erosion process of the carriers. Thus a drug depot effect could be achieved by the carriers, which could act as a barrier against diffusion of hydrophobic drugs (Liu et al., 2016). The insoluble drugs loaded in the carriers may show a stable state and slow drug release over a prolonged period of time. The release rate of T-PNPs was the slowest: this may due to the sustained effect of the polymeric materials (Wang et al., 2015). The release of the T-SLNs was relatively faster than T-NLCs: This may due to the out-layer of NLCs hindered the release of TMZ (Gaba et al., 2015). The sustained release

can be beneficial for drugs with irritation effects at high concentrations (Feng et al., 2014). This release behavior was highly advantageous to targeted cancer therapy since the amount of drug released prematurely might be minimized during circulation in the bloodstream, thereby providing an enough amount of drug to effectively kill the cancer cells once the carriers were internalized via endocytosis (Gao et al., 2015). The sustained release behavior of the carriers may give continuous protection of the drug and lead to the persistent *in vitro* cytotoxicity and *in vivo* anti-tumoral therapeutic effect.

*In vitro* cytotoxicity of T-PNPs, T-SLNs, T-NLCs, and T-SOL was evaluated on U87 MG cells at different concentrations after 48 h of incubation. All drug containing formulations inhibited the growth cells over the studied concentrations and the toxicity conformed to a concentration-dependent pattern (Figure 5). T-PNPs, T-SLNs, and T-NLCs showed significantly higher cytotoxicity than T-SOL ($p < 0.05$). The $IC_{50}$ value of T-NLCs is less than T-SLNs and T-PNPs. The data indicate that T-NLCs are capable of killing GBM cells in culture much more effectively than T-SLNs and T-PNPs. This enhanced killing *in vitro* reflects the ability of the NLCs to enter the cancer cells and to deliver a payload (in this case TMZ) to them (Kim et al., 2015). T-NLCs showed the best ability in reducing the viability of malignant glioma cells, accounting for the highest anti-tumor activity.

*In vivo* anti-tumor efficiency of TMZ/DNA-NLCs was assessed via measuring the mean tumor volume ($mm^3$) and the inhibition of tumor growth in tumor-bearing mice (Figure 6). Although tumor growth was suppressed to some extent after the administration of T-SOL, while in contrast, tumor growth was significantly inhibited when nanocarrier formulations were administered intravenously. The most obvious tumor regressions were observed in the T-NLCs group, the tumor growth was prominently inhibited. These results indicate that tumor growth was significantly inhibited by T-NLCs ($p < 0.05$). The tumor growth inhibition rate of T-NLCs was the highest *in vivo*. The results suggested that the NLC formulations performed better than the SLNs and PNPs. These results *in vivo* are in accordance with the outcomes of the *in vitro* cytotoxicity studies. These may attribute to the better capacity of the NLCs to enter tumor tissues and deliver the drug to the cancer cells (Shi et al., 2013).

## Conclusion

To construct better TMZ-loaded nanocarriers for GBM chemotherapy, three kinds of nanocarriers, T-NLCs, T-SLNs, and T-PNPs, were prepared. T-NLCs exhibited significantly better ability in the *in vitro* and *in vivo* anti-tumor study. The NLCs prepared in this research could be applied as an effective tumor therapy strategy for treatment in malignant GBM. Future research may focus on the use of the NLCs loading other payloads for the treatment of GBM.

## Declaration of interest

The authors report no conflicts of interest. The authors alone are responsible for the content and writing of this work.

## References


Agirre M, Zarate J, Puras G, et al. (2015). Improving transfection efficiency of ultrapure oligochitosan/DNA polyplexes by medium acidification. Drug Deliv 22:100–10.

Anirudhan TS., Binusreejayan (2016). Dextran based nanosized carrier for the controlled and targeted delivery of curcumin to liver cancer cells. Int J Biol Macromol 88:222–35.

Barbu E, Molnàr E, Tsibouklis J, et al. (2009). The potential for nanoparticle-based drug delivery to the brain: overcoming the blood–brain barrier. Expert Opin Drug Deliv 6:553–65.

Boyles MS, Kristl T, Andosch A, et al. (2015). Chitosan functionalisation of gold nanoparticles encourages particle uptake and induces cytotoxicity and pro-inflammatory conditions in phagocytic cells, as well as enhancing particle interactions with serum components. J Nanobiotechnol 13:84.

Carbone C, Campisi A, Musumeci T, et al. (2014). FA-loaded lipid drug delivery systems: preparation, characterization and biological studies. Eur J Pharm Sci 52:12–20.

Chen Z, Lai X, Song S, et al. (2016). Nanostructured lipid carriers based temozolomide and gene co-encapsulated nanomedicine for gliomatosis cerebri combination therapy. Drug Deliv 23:1369–73.

Chekhonin VP, Baklaushev VP, Yusubalieva GM, et al. (2012). Targeted delivery of liposomal nanocontainers to the peritumoral zone of glioma by means of monoclonal antibodies against GFAP and the extracellular loop of Cx43. Nanomedicine 8: 63–70.

Chinaeke EE, Chime SA, Onyishi VI, et al. (2015). Formulation development and evaluation of the anti-malaria properties of sustained release artesunate-loaded solid lipid microparticles based on phytolipids. Drug Deliv 22:652–65.

Feng R, Zhang Z, Li Z, et al. (2014). Preparation and *in vitro* evaluation of etoposide-loaded PLGA microspheres for pulmonary drug delivery. Drug Deliv 21:185–92.

Frungillo L, Martins D, Teixeira S, et al. (2009). Targeted antitumoral dehydrocrotonin nanoparticles with L-ascorbic acid 6-stearate. J Pharm Sci 98:4796–807.

Gaba B, Fazil M, Ali A, et al. (2015). Nanostructured lipid (NLCs) carriers as a bioavailability enhancement tool for oral administration. Drug Deliv 22:691–700.

Gao H, Yang Z, Cao S, et al. (2014). Tumor cells and neovasculature dual targeting delivery for glioblastoma treatment. Biomaterial 35: 2374–82.

Gao Y, Zhang C, Zhou Y, et al. (2015). Endosomal pH-responsive polymer-based dual-ligand-modified micellar nanoparticles for tumor targeted delivery and facilitated intracellular release of paclitaxel. Pharm Res 32:2649–62.

Gastaldi L, Battaglia L, Peira E, et al. (2014). Solid lipid nanoparticles as vehicles of drugs to the brain: current state of the art. Eur J Pharm Biopharm 87:433–44.

Hejri A, Khosravi A, Gharanjig K, et al. (2013). Optimisation of the formulation of β-carotene loaded nanostructured lipid carriers prepared by solvent diffusion method. Food Chem 141:117–23.

Hou LC, Veeravagu A, Hsu AR, et al. (2006). Recurrent glioblastoma multiforme: a review of natural history and management options. Neurosurg Focus 20:E5.

Huang G, Zhang N, Bi X, et al. (2008). Solid lipid nanoparticles of temozolomide: potential reduction of cardial and nephric toxicity. Int J Pharm 355:314–20.

Jain KK. (2010). Advances in the field of nanooncology. BMC Med 8: 83.

Khan AW, Kotta S, Ansari SH, et al. (2015). Self-nanoemulsifying drug delivery system (SNEDDS) of the poorly water-soluble grapefruit flavonoid Naringenin: design, characterization, *in vitro* and *in vivo* evaluation. Drug Deliv 22:552–61.

Kim SS, Harford JB, Pirollo KF, et al. (2015). Effective treatment of glioblastoma requires crossing the blood–brain barrier and targeting tumors including cancer stem cells: the promise of nanomedicine. Biochem Biophys Res Commun 468:485–9.

Kumar A, Ahuja A, Ali J, et al. (2016). Curcumin-loaded lipid nanocarrier for improving bioavailability, stability and cytotoxicity against malignant glioma cells. Drug Deliv 23: 214–29.

Liu Y, Gao D, Zhang X, et al. (2016). Antitumor drug effect of betulinic acid mediated by polyethylene glycol modified liposomes. Mater Sci Eng C Mater Biol Appl 64:124–32.

Martins SM, Sarmento B, Nunes C, et al. (2013). Brain targeting effect of camptothecin-loaded solid lipid nanoparticles in rat after intravenous administration. Eur J Pharm Biopharm 85:488–502.

Moghimi SM, Hunter AC, Murray JC. (2001). Long-circulating and target-specific nanoparticles: theory to practice. Pharmacol Rev 53: 283–318.

Müller RH, Shegokar R, Keck CM. (2011). 20 years of lipid nanoparticles (SLN and NLC): present state of development and industrial applications. Curr Drug Discov Technol 8:207–27.

Puglia C, Offerta A, Tirendi GG, et al. (2016). Design of solid lipid nanoparticles for caffeine topical administration. Drug Deliv 23:36–40.

Shi F, Yang G, Ren J, et al. (2013). Formulation design, preparation, and *in vitro* and *in vivo* characterizations of β-Elemene-loaded nanostructured lipid carriers. Int J Nanomedicine 8:2533–41.

Song S, Mao G, Du J, et al. (2016). Novel RGD containing, temozolomide-loading nanostructured lipid carriers for glioblastoma multiforme chemotherapy. Drug Deliv 23:1404–8.

Tian XH, Lin XN, Wei F, et al. (2011). Enhanced brain targeting of temozolomide in polysorbate-80 coated polybutylcyanoacrylate nanoparticles. Int J Nanomedicine 6:445–52.

Tiwari R, Pathak K. (2011). Nanostructured lipid carrier versus solid lipid nanoparticles of simvastatin: comparative analysis of characteristics, pharmacokinetics and tissue uptake. Int J Pharm 415: 232–43.

Wang T, Zhao P, Zhao Q, et al. (2016). The mechanism for increasing the oral bioavailability of poorly water-soluble drugs using uniform mesoporous carbon spheres as a carrier. Drug Deliv 23: 420–8.

Wang W, Zhou F, Ge L, et al. (2012). Transferrin-PEG-PE modified dexamethasone conjugated cationic lipid carrier mediated gene delivery system for tumor-targeted transfection. Int J Nanomedicine 7:2513–22.

Wang Y, Li P, Chen L, et al. (2015). Targeted delivery of 5-fluorouracil to HT-29 cells using high efficient folic acid-conjugated nanoparticles. Drug Deliv 22:191–8.

Woodworth GF, Dunn GP, Nance EA, et al. (2014). Emerging insights into barriers to effective brain tumor therapeutics. Front Oncol 4:126.

Wu M, Fan Y, Lv S, et al. (2015). Vincristine and temozolomide combined chemotherapy for the treatment of glioma: a comparison of solid lipid nanoparticles and nanostructured lipid carriers for dual drugs delivery. Drug Deliv 1–6.

Zhang B, Sun X, Mei H, et al. (2013). LDLR-mediated peptide-22-conjugated nanoparticles for dual-targeting therapy of brain glioma. Biomaterials 34:9171–82.

Zhang J, Wang X, Liu T, et al. (2016). Antitumor activity of electrospun polylactide nanofibers loaded with 5-fluorouracil and oxaliplatin against colorectal cancer. Drug Deliv 23:794–800.

Zou W, Cao G, Xi Y, et al. (2009). New approach for local delivery of rapamycin by bioadhesive PLGA-carbopol nanoparticles. Drug Deliv 16:15–23.